LUMINESCENCE IMAGING OF EXTENDED DEFECTS IN SiC VIA HYPERSPECTRAL IMAGING

Joshua D. Caldwell[1,a,*], Laurent Lombez[2,b], Amaury Delamarre[2c], Jean-François Guillemoles[2,d], Brice Bourgoin[4,e], Brett A. Hull[3,f], Marc Verhaegen[4,g]

1. Naval Rasearch Laboratory, 4555 Overlook Ave, S.W. Washington, D.C. 20375, USA
2. Chimie ParisTech, École nationale supérieure, 11, rue Pierre et Marie Curie, 75231 Parie, France
3. Cree Inc., E. Corwallis Rd., Research Triangle Park, NC 27709
4. Photon etc., 5795 avenue De Gaspé, #222, Montréal, Québec, H2S 2X3, Canada

ABSTRACT

Over the past decade, improvements in silicon carbide growth and materials has led to the development of commercialized unipolar devices such as Schottky diodes and MOSFETs, however, much work remains to realizing the goal of wide-scale commercialization of both unipolar and bipolar devices such as pin diodes or IGBTs, for high applications requiring high powers, operating in elevated temperatures or radiation environments or for many fast switching applications. Despite the great strides that have been made in reducing extended and point defect densities during this period, such defects still remain and with the push to lower off-cut angle substrates are in many cases seeing increases in prevalence. Thus, spectroscopic and imaging techniques for locating and identifying these defects are in high demand. Luminescence imaging and spectroscopy have both been utilized heavily in such work, yet simultaneously obtaining corresponding spectroscopic and spatial information from such defects is problematic. Here we report on hyperspectral imaging of electroluminescence from SiC pin diodes, whereby a stack of luminescence images are collected over a wide spectral range (400-900 nm), thereby providing the ability to both image distinct features and identify their corresponding spectral properties. This process is also equally applicable to collecting either photo- or electroluminescence from other materials or devices emitting in either the UV-Vis or NIR spectral range, as well as to reflectance, transmission or other imaging techniques.

HYPERSPECTRAL IMAGING

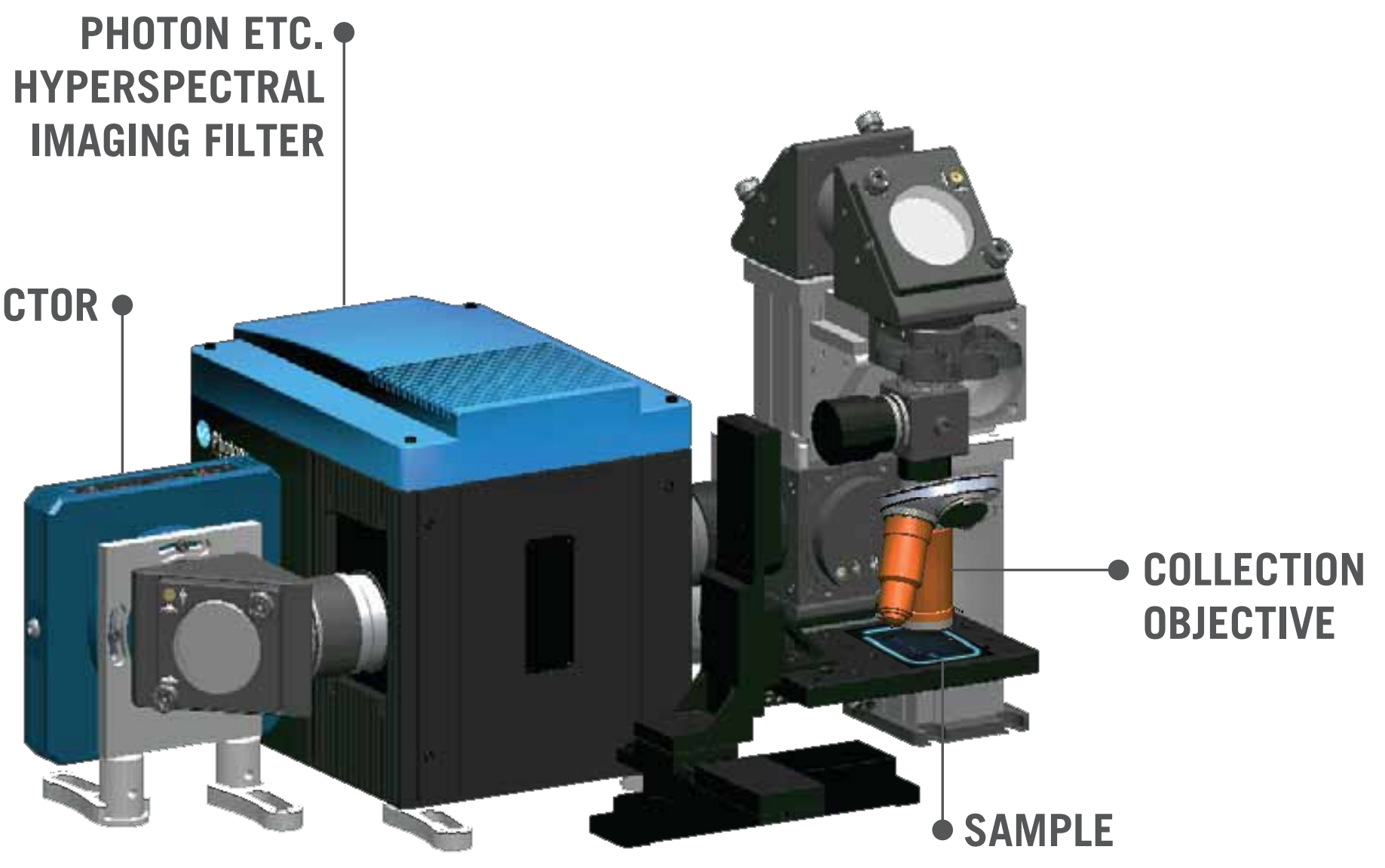

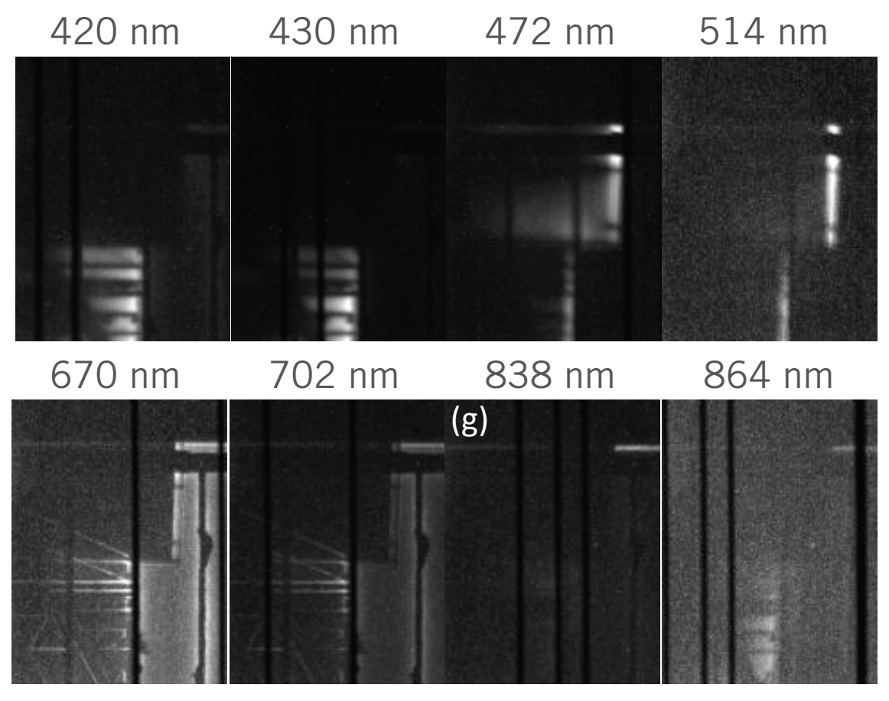

Electroluminescence (EL) was induced via driving ~28A/cm^2 through 0.93x0.93 mm pin diode. EL was collected 20x 0.4 NA objective. A series of reflecting mirrors focused the EL onto the entrance slit of the hyperspectral imaging filter. By rotating the two volume Bragg gratings with respect to the incident, the output from the filter was narrowed to 2 nm, with the center wavelength of this pass-band varied from 400-900 nm. This output was focused onto a thermoelectrically cooled CCD detector. Images were collected in 2 nm increments for 30s each. The collection of images were stacked and a rectification process was performed that enables a spectrum from any given feature within the structure to be obtained, thereby providing direct correlation between given structural features and their corresponding spectra within a singleacquisition set.

REAL COLOR IMAGING

REAL COLOR EL IMAGING

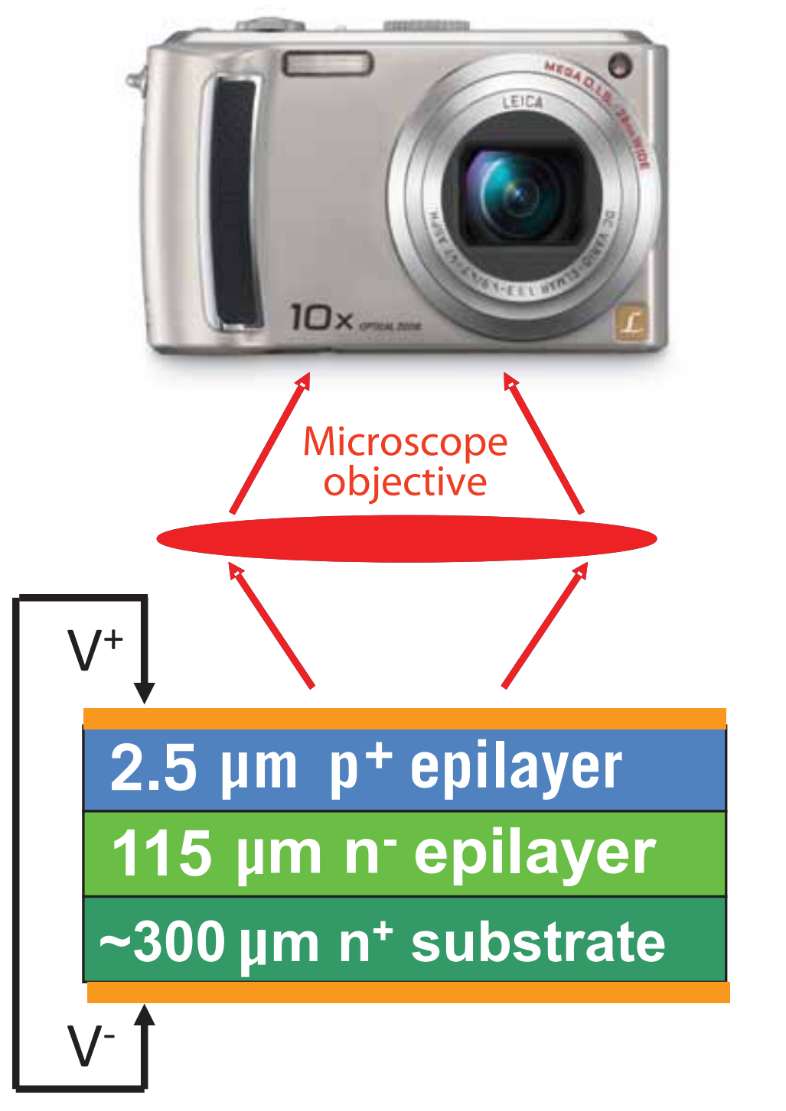

- Forward-bias injection of ehp induces EL
- EL Collected through 10X 0.25NA, 20x0.4 NA and 50x 0.7 NA objectives
- Imaging 1-10s Olympus 750 UltraZoom – 'real-color' imaging

REAL COLOR EL OF PiN DIODES

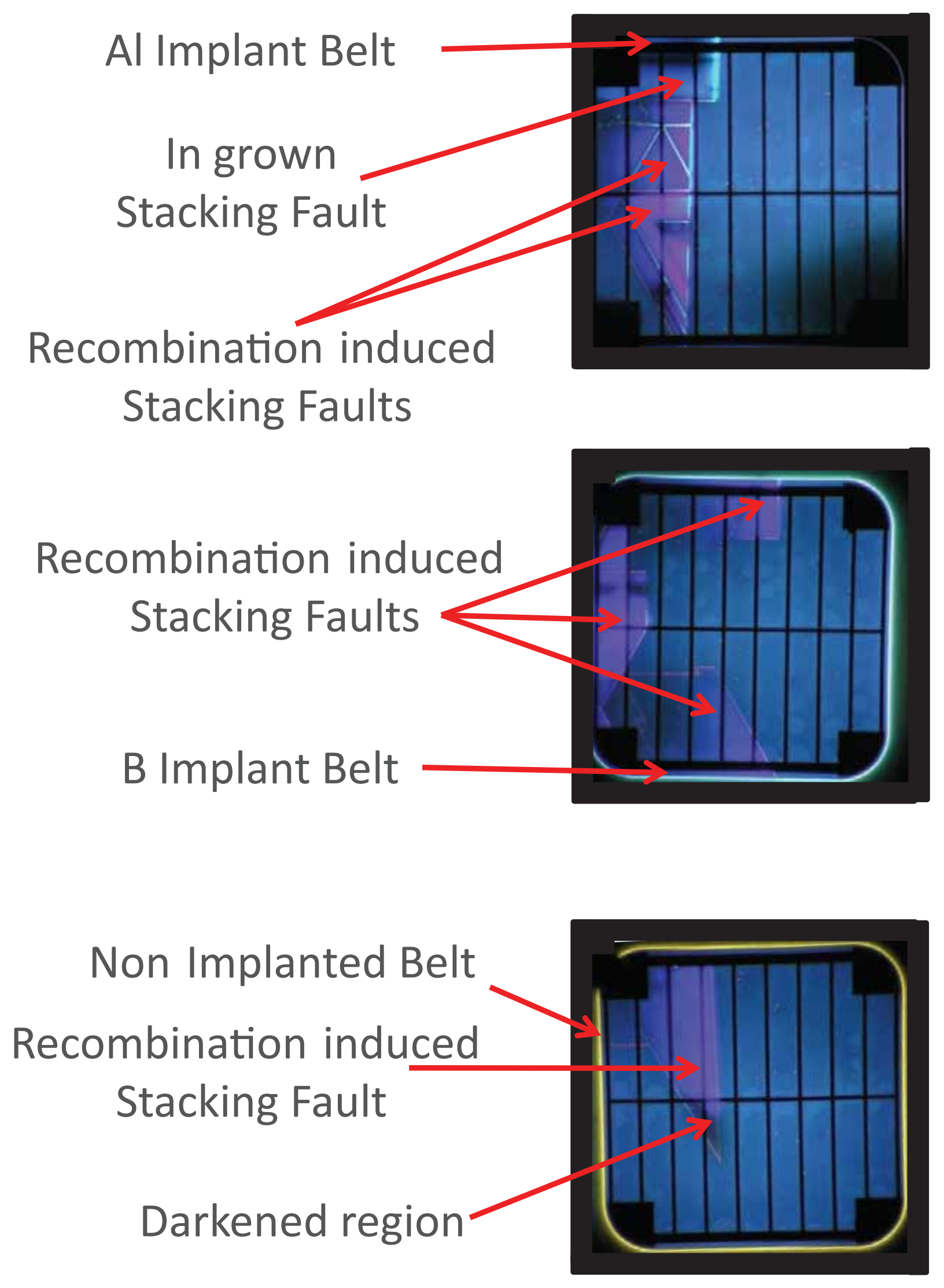

RECOMBINATION-INDUCED STACKING FAULTS

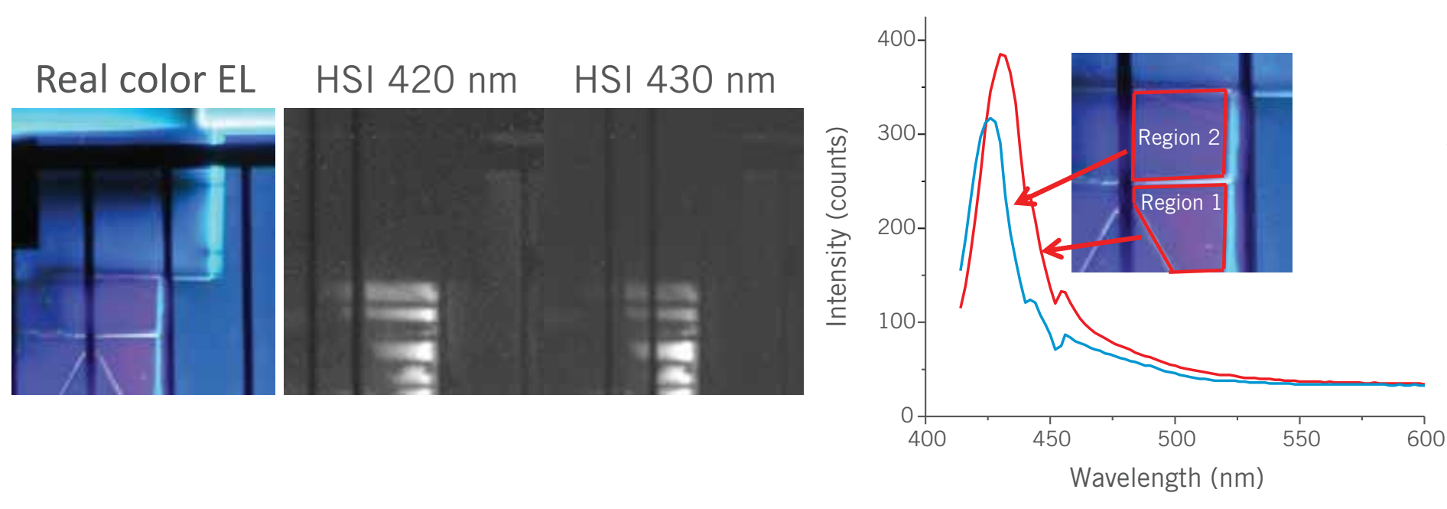

- Two regions within area of overlapping SFs separated by partial dislocation
- Region with higher density of overlapping SFs
- Shift in the peak response of ~ 5 nm (30 meV)
- Broader linewidth and higher intensity emission

IMPLANT-INDUCED DEFECT BANDS

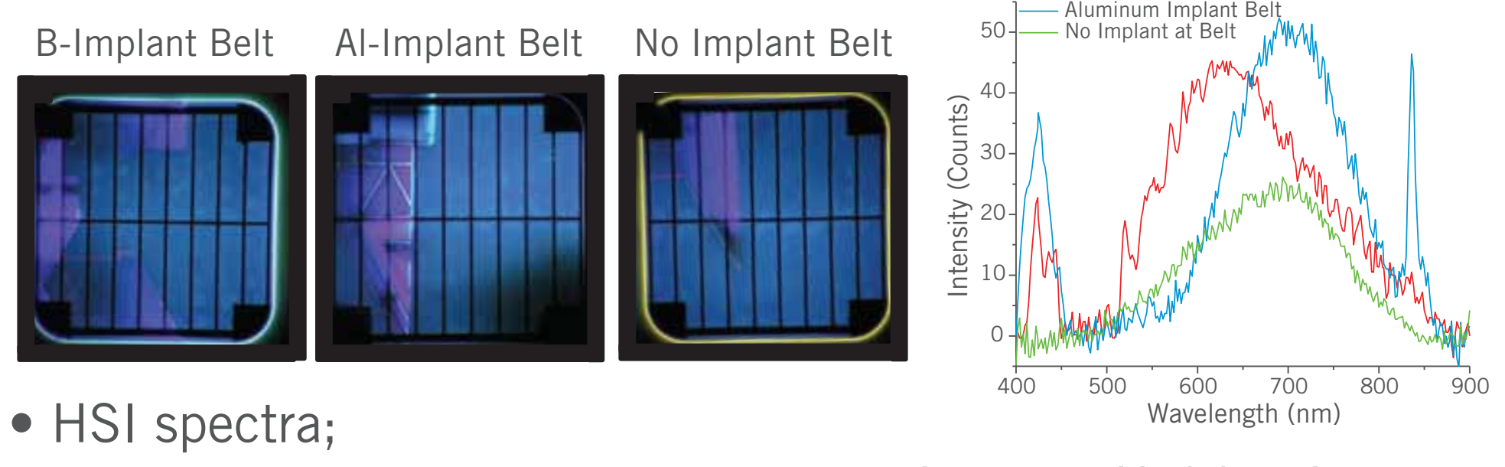

- Implants in 'belts' surrounding diodes
- Real Color EL indicates that the belts emit differently
  - Boron implant belt → greenish-yellow hue
  - Aluminum implant belt → dull blue hue
  - No implants → bright yellow belt
- HSI spectra;
  - Boron Implant belt → peak near 645 nm (1.92 eV) and ~700 nm
  - Aluminum Implant Belt → peak near 700 nm and sharp peak at 836 nm (1.48 eV)
  - No implants → peak near 700 nm; potentially a short wavelength shoulder
  - All spectra feature 700 nm feature → intrinsic defect within the belt region perhaps due to mesa etch process
  - Origin of 645 nm (Boron) or 836 nm (Aluminum) emission is unclear

IN-GROWN STACKING FAULTS

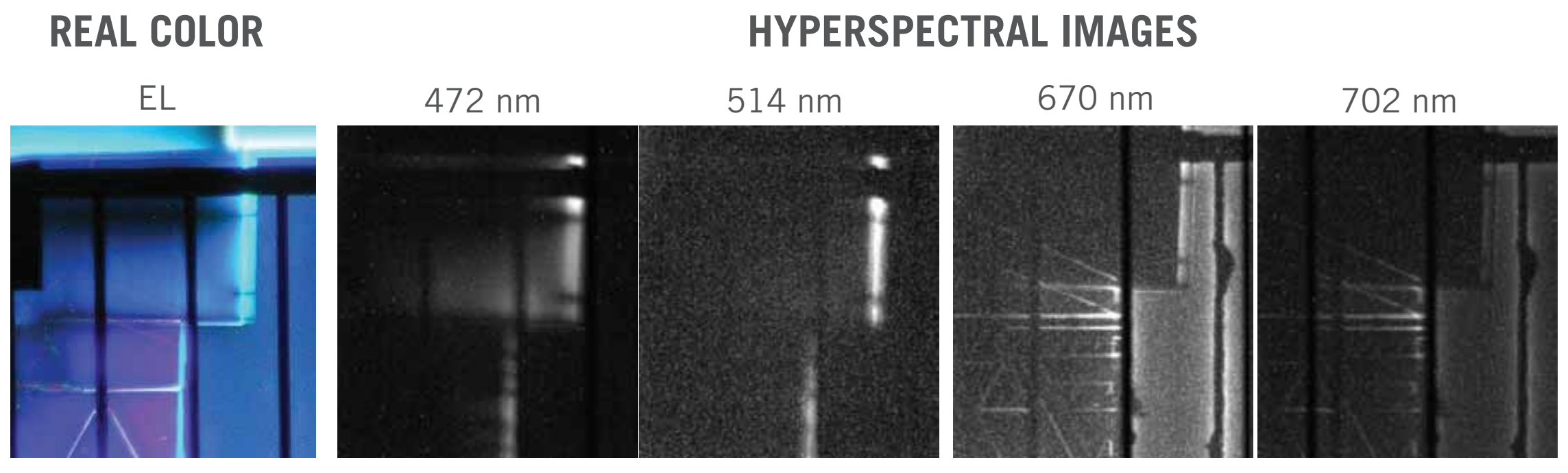

- In-grown stacking faults exhibit two emission regions
- Body of fault gives off deep blue EL
- Rectangular region near right edge of fault emits a teal color
- Rectangular region emits over a broader range
- Appears to be region where SF penetrates into pn junction at top of diode

IN-GROWN STACKING FAULTS: INFLUENCE OF PN JUNCTION

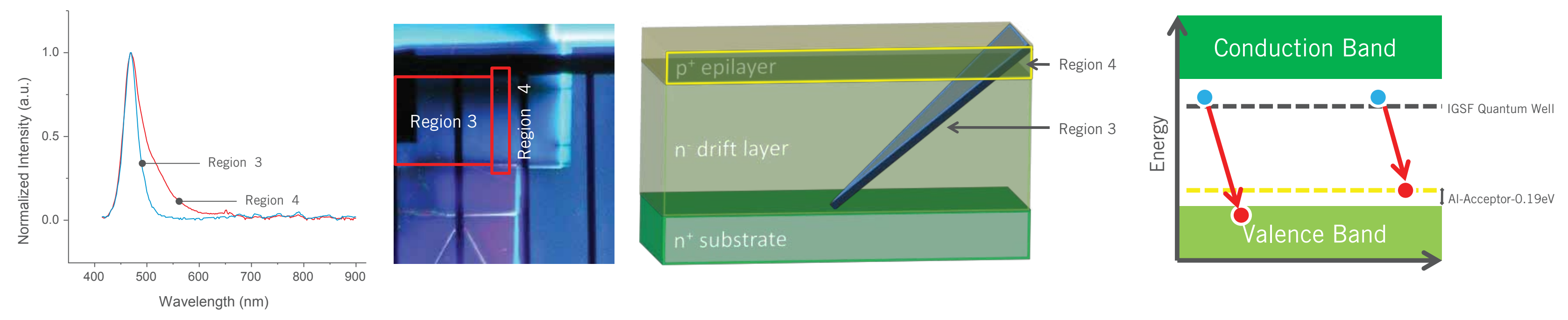

- Rectangular region (Region 4) is where IGSF penetrates pn junction
- Additional recombination pathway exists:
  - Preferred Pathway → e⁻ trapped in IGSF recombine with h⁺ in VB
  - Alternate Pathway → e⁻ trapped in IGSF recombine with non-ionized h⁺ at acceptor levels
  - Consistent with observations of Caldwell et al. APL 89, 103519 (2006), where IGSFs exhibited bright EL and PL at surface and anticipated to be due to recombination at acceptors

IN-GROWN STACKING FAULTS: HSI IDENTIFICATION OF IGSF STACKING ORDER

APPLIED PHYSICS LETTERS 94, 092101 (2009)

CATHODOLUMINESCENCE STUDY OF THE PROPERTIES OF STACKING FAULT IN 4H-SiC HOMOEPITAXIAL LAYERS

Serguei I. Maximenko,[1a)] Jaime A. Freitas, Jr.[1] Paul B. Klein,[1] Amitesh Shrivastava,[2] and Tangali S. Sudarshan[2]

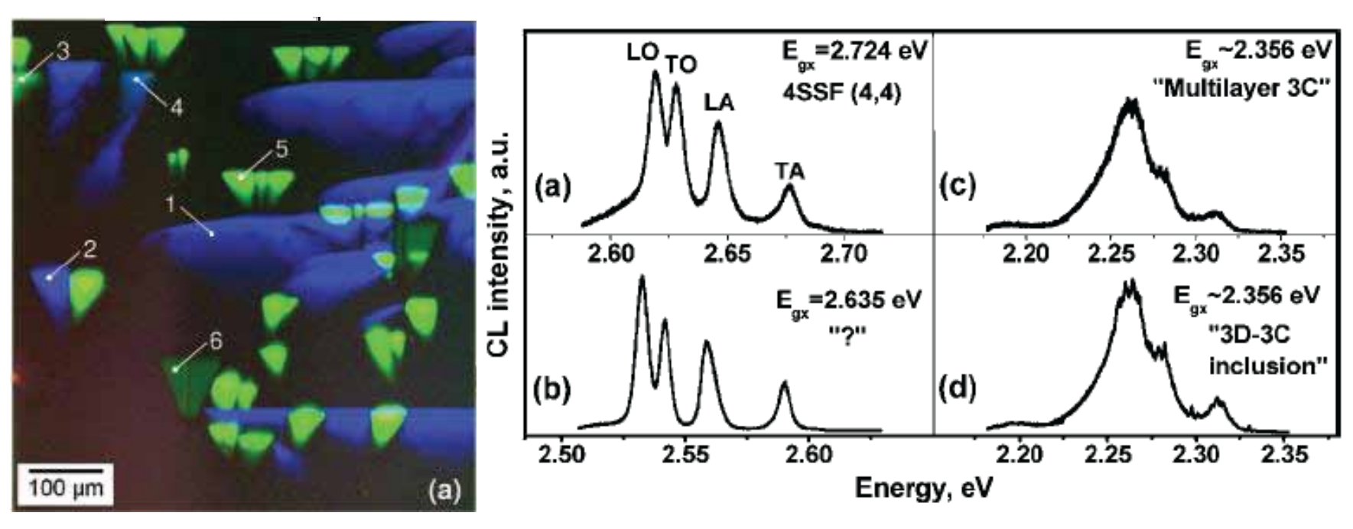

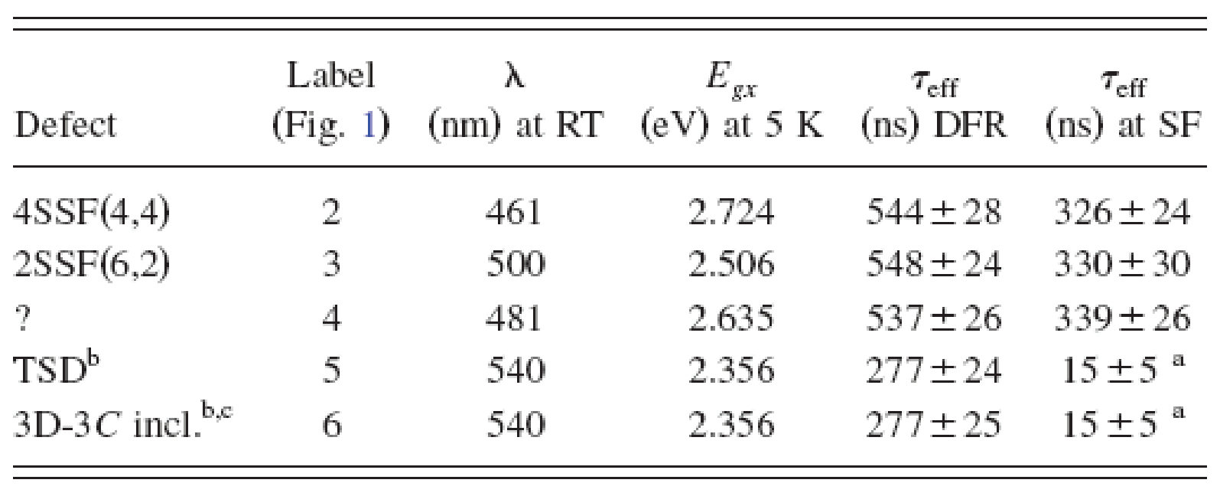

Defect	Label (Fig. 1)	λ (nm) at RT	E_{gx} (eV) at 5 K	τ_{eff} (ns) DFR	τ_{eff} (ns) at SF
4SSF(4,4)	2	461	2.724	544 ± 28	326 ± 24
2SSF(6,2)	3	500	2.506	548 ± 24	330 ± 30
?	4	481	2.635	537 ± 26	339 ± 26
TSD[b]	5	540	2.356	277 ± 24	15 ± 5 [a]
3D-3*C* incl.[b,c]	6	540	2.356	277 ± 25	15 ± 5 [a]

- IGSF studied here had primary emission of 2.64 eV at room temperature
- Previous work by Maximenko et al. established
  - 4 bilayer IGSF (4,4 in Zhdanov notation) emits at 2.61 eV
  - Have a right triangular shape
  - This corresponds to an excitonic band gap of 2.724 eV
- All results are consistent with our EL hyperspectral imaging work now
- Illustrates that HSI technique can be used to identify specific defects

CONCLUSIONS

Here we have reported on the use of hyperspectral electroluminescence imaging for simulaneously obtaining correlated spatial and structural information from extended defects within SiC pin diodes. Using this technique, the spectral and spatial properties of several defects including recombination induced stacking faults (SFs), partial dislocations, defect levels associated within Al and B implanted regions and an in-grown stacking fault (IGSF) were identified and studied. In the case of the SFs, it was determined that in addition to the widely-reported emission near 426 nm, an additional emission band is induced at a position 30 meV deeper (~430 nm) was also induced in regions with a large number of overlapping SFs. The reason for this shift is still being explored. Additional defect levels with emission energies of 1.48 and 1.71 eV were observed in the regions of an Al and B implant belts, respectively. Finally, EL spectra from a (4,4) IGSF in Zhdanov notation exhibited two emission lines. The primary line was centered at approximately 2.64 eV, which is consistent with IGSF quantum well to valence band recombination. The second emission, observed as a shoulder in the spectra collected from the rectangular region where the IGSF meets the surface of the diode, was centered at 0.18 eV below the primary emission line and is consistent with recombination between electrons in the IGSF with holes at the acceptor levels. These efforts indicate that hyperspectral imaging can provide a unique methodology for simultaneously identifying the presence, spatial extent, location and spectral properties of extended defects in both wide and narrow-band gap semiconductor devices.